Response to Reviewer #2

We sincerely thank the reviewer for the thorough evaluation of our manuscript and for the positive assessment of our work. The constructive comments and valuable suggestions have helped us identify several areas where the manuscript can be further improved in terms of clarity, interpretation, and technical rigor.

We have carefully addressed each comment point by point in the following responses. All corresponding revisions have been incorporated into the manuscript and are clearly marked in the revised version.

General Comments

This study presents an ensemble machine learning (EML)–based aerosol retrieval algorithm for estimating both aerosol optical and microphysical properties from ground-based Sun–sky photometer measurements. The results demonstrate performance comparable to AERONET operational products, while achieving a computational efficiency improvement of more than five orders of magnitude. The authors also clearly describe the limitations of the current approach. Overall, the manuscript is well organized, with appropriate and informative figures and tables. Therefore, this work is relevant to the AMT readership and fits well within the journal's scope. I recommend publication after minor revision. However, the manuscript would benefit from a more in-depth interpretation of the results, rather than primarily repeating quantitative evaluation metrics that are already evident from the figures and tables. In addition, although a 5% radiance uncertainty is assumed based on earlier studies, it would be valuable to discuss whether this assumption remains valid given current state-of-the-art radiative transfer calculations and instrumental capabilities.

Response:

Thank you for your constructive and inspiring comments. When discussing algorithm inversion results, we should not only look at the data, but also analyze the physical mechanisms reflected behind it. Specifically, we have added a discussion on the possible reasons behind the ability of multi input/output models to distinguish specific wavelength observations and simultaneously utilize multi wavelength observations. The 5% radiance uncertainty adopted in this study follows commonly used assumptions in previous Sun–sky photometer retrieval studies and AERONET-related algorithms, where typical sky radiance uncertainties are reported to be on the order of 3–5%, while direct solar measurements are often within 1–2%. With improvements in instrument calibration and radiative transfer modeling, the actual uncertainty for high-quality observations may be lower under ideal conditions. Therefore, the 5% assumption can be considered a conservative estimate. In our framework, this uncertainty level is used to ensure that the model remains robust under realistic observational noise and does not overfit idealized noise-free simulations. The 5% residual may also come from other factors involved in radiative transfer calculations, such as solar incident radiation at the top of the atmosphere, surface albedo, gas absorption, and Rayleigh scattering. The setting of observation error covariance matrix is crucial for iterative statistical algorithms based on Bayesian optimization. However, for machine learning algorithms, a 5% observation uncertainty does not affect the aerosol parameter inversion results, but only evaluates the model in radiation space. The smaller the residual between the radiation calculated by simulating the aerosol parameters using inversion and the observation, the more accurate the inversion results are. We must admit that compared to statistical algorithms, machine learning models are difficult to provide posterior errors. We estimate the propagation error through multiple perturbations (Section 2.4), and whether to choose a perturbation intensity of 5% also affects the error evaluation of the inversion results. Excessive perturbation intensity may overestimate the error, but currently there is no particularly scientific method to find a more suitable value. We have added discussion explanations in Section 3.4: *According to Section 2.4, the evaluation of propagation error depends on the intensity of perturbation to the input radiation. The stronger the perturbation, the greater the error. In the future, the accuracy of the instruments will likely improve, and we hope to achieve better accuracy in the inversion results.*

Specific Comments

Reviewer Comment #1:

220 # --> n or n* etc, otherwise please define #

Response:

Thank you for pointing out that we did miss the definition of # in the formula (11). The following discussion has been added to the main text: *# is a counting symbol representing the number of points in the subsequent set.* The condition that a set element needs to satisfy is that the absolute deviation between y and $\hat{y}$ is less than the specified uncertainty.

Reviewer Comment #2:

262 how do you make sure these results are without overfitting?

Response:

We fully agree with your point of view that preventing overfitting in model training is an issue that must be considered in machine learning model training. On one hand, our model was trained on a dataset of 100,000 sets of simulated radiative transfer patterns. During the training process, 5% of the data will not participate in the optimization of the model's structural parameters, but will be used to monitor whether the model is overfitting. After each round of training, the model needs to make predictions on this 5% of the data, and the loss function between the predicted values and the ground truth should not have a significant upward trend. If the loss function changes too little or shows a significant upward trend compared to the previous two rounds of training, the training will be terminated. On the other hand, when designing hyperparameters for the EML model, we will minimize the model complexity as much as possible. For example, the number of decision trees in the Random Forest model should not be too many, and the number of network layers and neurons in the Multi-Layer Perceptron should not be too many. Thirdly, the prediction performance of the model on training set, validation set and test set has not significantly deteriorated or improved. The validation set is comprised of simulated data that did not participate in model training, while the test set is derived from real observations from a photometer.

Reviewer Comment #3:

284-286 please suggest that these results are faster by O(10^5), for example, as stated in the Summary section.

Response:

We should indeed further clarify the magnitude of the speed increase in lines 333-335 in the revised manuscript, which has been revised in the manuscript: *It requires only 0.18 milliseconds to invert a single measurement, which corresponds to a speed improvement on the order of* 10^5*, since traditional numerical retrieval algorithms often take several minutes per case.* But we acknowledge that the speed improvement of inversion algorithms cannot be estimated by specific values, because for traditional iterative optimization algorithms, the number of iteration steps and radiation transfer calculations required for different cases are different, usually taking minutes. For the EML-based inversion algorithm, the speed is also affected by computer computing power, but the inversion of a case is in milliseconds. Therefore, the fold increase in inversion speed is approximately on the order of 10^5.

Reviewer Comment #4:

323 For example, why 440 nm radiance has such high impact in determining SSA? With stronger Rayleigh scattering, the presence of absorbing aerosol shows larger difference…e.g. similarly for g as well, and throughout the following explanations.

Response:

Thank you very much for your suggestion. We should not only explain the data, but also increase our consideration of physical laws. Firstly, we have made adjustments to Figure 4 in the revised manuscript, mainly by refining the spectral AOD feature and displaying the importance of the AOD features for each of the four observation bands. For the inversion of 440nm SSA, the most important input variables are the AOD and radiance observed by the photometer at 440nm. AOD is obtained by direct observation with a photometer, which characterizes the total column amount of aerosols along the entire optical path, including the absorption extinction and scattering extinction of aerosols. The radiance observed in Almucantar mode is mainly sky scattered light, and the path length of scattered light will be significantly different from direct light. The absorption and scattering characteristics of aerosols in the atmosphere will significantly affect the observed radiation signal. Therefore, the radiance observed from different angles is crucial for the inversion of SSA and g.

The revised manuscript has added Tables 2 and 3, which provide a detailed list of variables that are simultaneously input or output to the EML. In Figure 4, it can be seen that the EML model effectively extracts and utilizes observation data from specific wavelength bands for aerosol parameter inversion at corresponding wavelengths. That is to say, the multi variable input-output EML model can learn wavelength sensitivity. As you said, Rayleigh scattering is stronger at shorter wavelengths, and absorbing aerosols such as black carbon and brown carbon are more sensitive in the blue light band. The sensitivity of SSA and g at 440nm to radiation at 440nm is stronger than that at longer wavelengths. The following discussion has been added in lines 376-379: *Rayleigh scattering is stronger at shorter wavelengths, and absorbing aerosols such as black carbon and brown carbon more heavily impact the blue light band. The* *sensitivity of SSA and g at 440nm to radiation at 440nm is stronger than in longer wavelength bands.* Another question is why the inversion parameters of one wavelength band are also affected by other wavelengths. *The three parameters g, r_{eff} and FMF essentially reflect the particle size distribution of aerosols, and this microphysical property will inevitably affect radiation transmission at multiple wavelengths.*

Table 2. Input variables of the EML Model

Input Variables	Count	Notes
Solar zenith angle	1	Equal to the viewing zenith angle, and the actual input is the cosine value of the angle.
Spectral AOD	4	AOD of four observation bands (440, 675, 870 and 1020 nm)
Radiance at 440nm	23	Defined at 23 relative azimuth angles (7°, 8°, 10°, 12°, 14°, 16°, 18°, 20°, 25°, 30°, 35°, 40°, 45°, 50°, 60°, 70°, 80°, 90°, 100°, 120°, 140°, 160°,180°)
Radiance at 675nm	23	Defined at 23 relative azimuth angles
Radiance at 870nm	23	Defined at 23 relative azimuth angles
Radiance at 1020nm	23	Defined at 23 relative azimuth angles
Observation geometries	23	Defined as the cosine value of the scattering angle between the incident sunlight and the observation direction of the photometer: $\cos(\theta_{sca}) = \cos(\theta_{sza})\cos(\theta_{vza}) + \sin(\theta_{sza})\sin(\theta_{vza})\cos(\theta_{raa})$. For Almucantar diffused sky radiation observations parallel to the horizontal plane, there is only one solar zenith angle and one viewing zenith angle in one scan, and the two angles are equal.

Table 3. Output variables of the EML Model

Output variables	Count	Notes
Spectral SSA	4	Single scattering albedo of aerosols in four observation bands
Spectral g	4	Scattering asymmetric factor of aerosol in four observation bands
Effective radius r_{eff}	1	Characterize the particle size of the aerosol group in the atmosphere column
Fine mode fraction FMF	1	Characterization of the volume proportion of fine particles (with a radius less than 1 micron) in the aerosol group in the atmospheric column

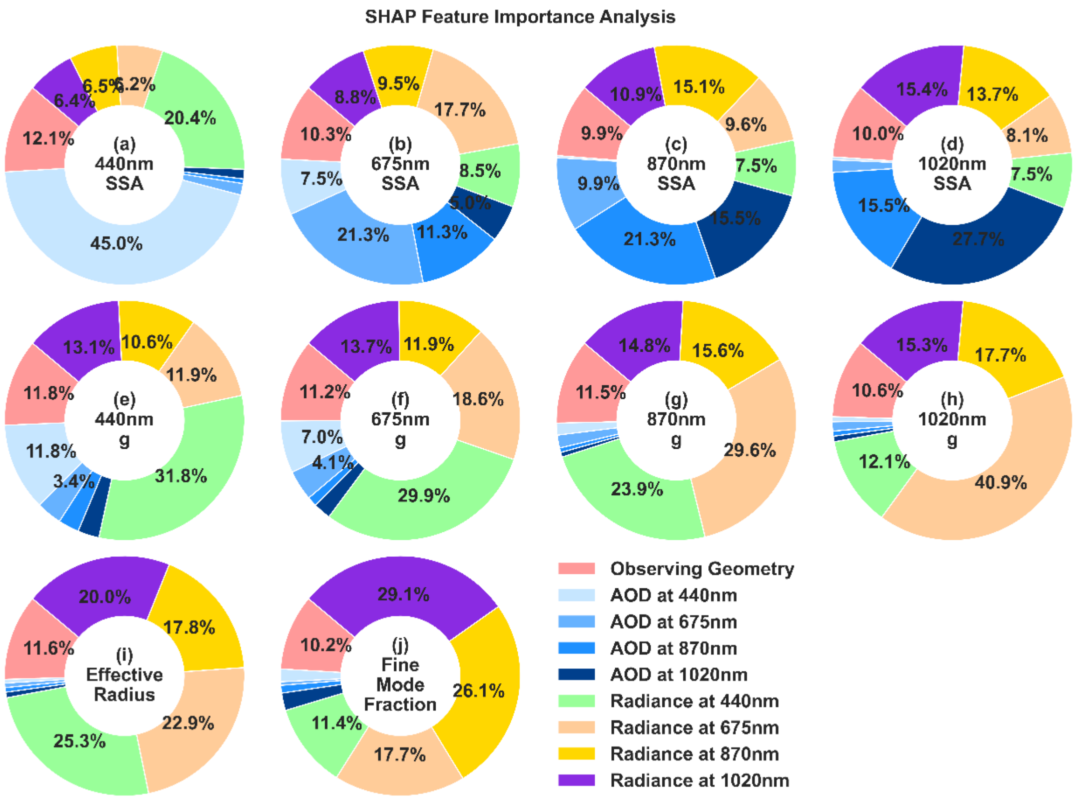

Figure 4. Importance analysis of input features based on SHAP values. Subfigures a-d correspond to retrieved variables SSA, e-h correspond to retrieved variables g, i correspond to r_{eff}, and j correspond to FMF. The four columns represent the observation wavelengths of 440, 675, 870, and 1020 nm in the first two rows. All 120 input features of the EML model are grouped into categories. Observation geometry includes the cosine of SZA and the scattering angle from the Almucantar scanning mode. Radiance refers to measured sky radiances from 23 observation geometries. Values less than 3% are hidden.

Reviewer Comment #5:

331, 407, 411 SCAs has this acronym defined earlier? I cannot find.

Response:

Sorry, it was indeed an omission in article writing process. SCA refers to "*the scattering angle*" and has been defined in the manuscript.

Reviewer Comment #6:

382-394 What is the reason to have lower performance for coarse particles as compared to fine particles, other than non-sphericity? Less number of training dataset? Please elaborate a little bit more.

Response:

We agree that non-sphericity alone may not fully explain the relatively lower retrieval performance for coarse particles, and we have expanded the discussion accordingly in the revised manuscript.

First, coarse-mode aerosols, such as dust and sea salt, are often significantly non-spherical. Radiative transfer calculations in many operational and machine-learning-based retrieval frameworks are typically based on Mie theory or spherical assumptions, which cannot fully reproduce the angular scattering patterns of irregular particles. As shown in previous studies (Dubovik et al., 2006), particle non-sphericity can substantially modify phase functions and polarization signals, especially in the coarse mode. In forward radiative transfer modeling, the T-matrix method—while capable of handling non-spherical particles—still faces limitations when it comes to accurately representing the scattering phase matrix of multi-faceted, multi-angle particles, which are approximated as ellipsoids (Mishchenko et al., 1996). This increases forward-model errors and reduces the uniqueness of the inverse solution, thereby degrading retrieval performance. In addition to non-sphericity, several other factors may contribute to the lower performance for coarse particles. (1) The radiative sensitivity of Sun–sky photometer measurements to coarse-mode microphysical variations is generally weaker than for fine-mode particles, particularly in forward scattering geometries, which reduces the information content available for inversion. Non-spherical scattering has higher asymmetry, far beyond forward and backward asymmetry, while ground-based photometers receive more forward scattering signals. (2) Strong parameter coupling among coarse-mode effective radius, volume concentration, and asymmetry factor may increase the ill-posedness of the inverse problem. (3) The distribution of training samples may also play a role, as coarse-mode-dominated cases are typically less frequent than fine-mode-dominated cases in ground-based observational datasets, potentially limiting the representation of extreme coarse regimes in the training process. We have now clarified these aspects in the revised manuscript to provide a more comprehensive interpretation of the observed performance differences.

The discussion added to the manuscript is as follows: *In addition, strong parameter coupling among coarse-mode effective radius, volume concentration, and asymmetry factor may increase the ill-posedness of the inverse problem. The distribution of training samples may also play a role, as coarse-mode-dominated cases are typically less frequent than fine-mode-dominated cases in observational datasets, potentially limiting the representation of extreme coarse regimes in the training process.*

Finally, thank you again for providing all the review comments, which helped me further consider and improve the algorithm design and manuscript content.

Reference:

Dubovik, O., Sinyuk, A., Lapyonok, T., Holben, B. N., Mishchenko, M. I., Yang, P., Eck, T. F., Volten, H., Muñoz, O., Veihelmann, B., van der Zande, V. J., Leon, J.-F., Sorokin, M., and Slutsker, I.: The application of spheroid models to account for aerosol particle nonsphericity in remote sensing of desert dust, J. Geophys. Res.-Atmos., 111, D11208, https://doi.org/10.1029/2005JD006619, 2006.

Mishchenko, M. I., Travis, L. D., Mackowski, D. W.: T-Matrix Computations of Light Scattering by Non-spherical Particles: A Review, J. Quant. Spectrosc. Radiat. Transfer, 55, 535–575, https://doi.org/10.1016/0022-4073(96)00002-7 , 1996.